Journal of Archaeological Science (1996) **23,** 95–107

Comparative Morphometric Study of a Human Phalanx from the Lower Pleistocene Site at Cueva Victoria (Murcia, Spain), by means of Fourier Analysis, Shape Coordinates of Landmarks, Principal and Relative Warps

P. Palmqvist and J. A. Pérez-Claros

Área de Paleontología, Departamento de Geología y Ecología, Facultad de Ciencias, Universidad de Málaga, E-29071 Málaga, Spain

J. Gibert and J. L. Santamaría

Institut Paleontològic "Dr M. Crusafont", Carrer de l'Escola Industrial 23, E-08201 Sabadell, Barcelona, Spain

(*Received 27 July 1994, revised manuscript accepted 11 October 1994*)

The presence of *Homo* in Europe longer than a million years ago is often discussed. The finding of a Lower Pleistocene phalanx from the karstic site of Cueva Victoria in Murcia (Spain) can contribute important information about this theme if the *Homo* identification is confirmed. We have used an array of morphometric analyses to study this phalanx, and to compare it with human, gorilla and cercopithecid phalanges. The morphometric variates included conventional distance and surface area measurements estimated from radiographs of the phalanges, harmonic amplitudes from Fourier series fitted to their contours, and shape coordinates of landmarks. Discriminant analysis was used to compare the groups, and principal and relative warp analyses used to investigate the relative position of landmarks. Results obtained with all morphometric methods consistently indicated a human affinity for the fossil, and thus constitute further evidence of the presence of *Homo* sp. in the southern Iberian Peninsula during the Lower Pleistocene.

© 1996 Academic Press Limited

Keywords: MORPHOMETRY, FOURIER SERIES, SHAPE COORDINATES, PRINCIPAL AND RELATIVE WARP ANALYSES, DISCRIMINANT ANALYSIS, *HOMO*, LOWER PLEISTOCENE.

Introduction

Cueva Victoria is a karstic site located in the San Ginés of the Jara Mountains (Cartagena, Murcia, southeastern Spain). During the Plio-Pleistocene, the vertical karst, of Messinian origin, gave rise to cave openings to the exterior, which became filled with bone-bearing breccia. The presence of fossils in the cave is believed to be due to the activities of scavenging carnivores, particularly hyaenids. The geological features of the Cueva Victoria site were studied by Ferrández *et al.* (1989) and its taphonomic characteristics by Gibert *et al.* (1992). The site was dated to the Lower Pleistocene by association of the following taxa: *Pachycrocuta brevirostris, Dicerorhinus etruscus, Mammuthus meridionalis, Canis estruscus, Homotheriun latidens, Castillomys crusafonti, Apodemus mystacinus* and *Allophaiomys chelinei.*

In 1984, Pons Moyá found a phalanx (CV-0) (Figure 1) in the bone bearing breccia at Cueva Victoria, and attributed the fossil to *Homo* sp. (Pons Moyá, 1985). A morphological study (Gibert & Pons Moyá, 1984) was undertaken to differentiate the phalanx from other pentadactyl mammals, particularly carnivores and beavers, and a biometric comparison was done with primates and ursids (Gibert, Pons & Ruz, 1985). Using both anatomical data and conventional biometric parameters it was possible to discriminate the Cueva Victoria phalanx form those of cercopithecids (*Cercopithecus nictitans, Macaca silvana, Mandrillus sphinx* and *Papio hamadryas*), apes (*Gorilla gorilla, Pan troglodytes, Pongo pygmaeus* and *Hylobates* sp.), ursids (*Ursus spelaeus* and *Ursus arctos*), terrestrial and marine carnivores (*Indarctos vireti, Hyaena* sp. and *Phoca* sp.) and beavers (*Stenofiber gaegeri*). The Cueva Victoria phalanx was also compared with human specimens, both modern and fossil (described by Musgrave, 1971), and the results placed this fossil within the range of variation of *Homo*. Gibert & Pérez (1989) performed a canonical variates analysis (Reyment, Blackith & Campbell, 1984), using the distance measurements estimated in the previously cited works. This analysis

0305-4403/96/010095+13 $12.00/0

© 1996 Academic Press Limited

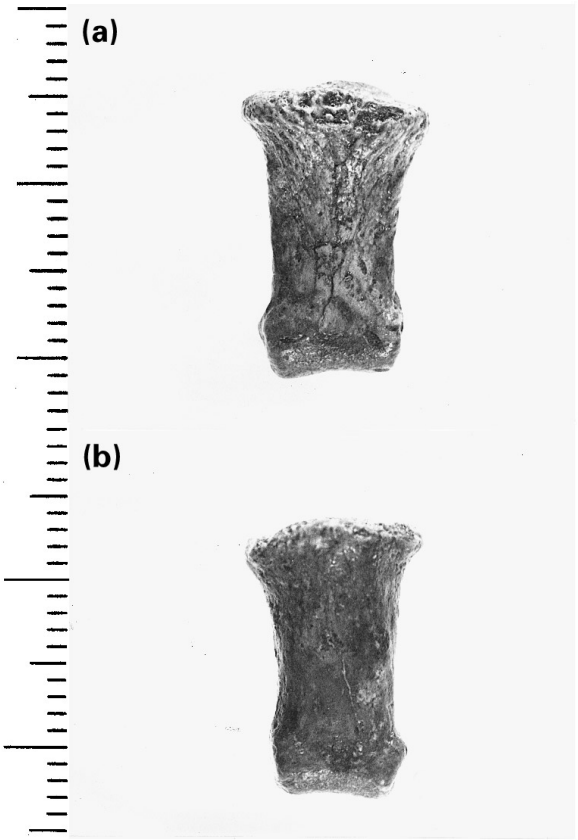

Figure 1. Human phalanx from the Lower Pleistocene karstic site of Cueva Victoria (Murcia, Spain): (a) palmar side, (b) dorsal side. Scale in mm.

allowed them to separate the fossil phalanx from phalanges of carnivores, cercopithecids and large-bodied pongids, and placed it firmly in the human sample.

The find in 1989 of an unworn crown of a second lower molar of a cercopithecid (*Theropithecus* cf. *oswaldi*) in Cueva Victoria (Gibert *et al.*, 1995) made further comparisons with these forms necessary, in order to separate CV-0 from large-bodied cercopithecids, given that previous work gave satisfactory results as regards discrimination from *Macaca* and pongids. In a radiological study, Santamaría & Gibert (1992) quantified several conventional parameters (distances and surface areas) estimated using image analysis techniques in radiographs of second phalanges of *Papio, Mandrillus* and *Homo sapiens sapiens*. They concluded that the Cueva Victoria phalanx could be separated from those of cercopithecids and attributed it to the genus *Homo*. As a methodological contrast, they also included foot phalanges of *Gorilla*, which are very similar to human ones (chimpanzee phalanges are rather different in shape). However, pongids became extinct in Europe during the Upper Miocene and were relegated to Africa and Asia; consequently, they have left no fossil traces in the European Plio-Pleistocene.

Few comparative studies of phalanges have been published, most descriptions being based on single specimens. The work of Musgrave (1969; 1971) is a noteworthy exception, and some of the methods used in the present study were based on approaches he described in his work, with Neanderthal phalanges.

In addition to the phalanx, two humeral fragments have been recovered in Cueva Victoria, and have been attributed to *Homo* sp. on the basis of anatomical features (Gibert *et al.*, 1992). Other European Lower Pleistocene remains have been found in the Venta Micena site (Orce, Granada, Spain), e.g. a juvenile cranial fragment and several humeral diaphyses, one of which is complete and probably belonged to the same individual as the skull. The hominid attribution of the cranial fragment has been established with anatomical (Gibert *et al.*, 1989), morphometric (fractal analysis of the sagittal and lambdoid sutures) (Gibert & Palmqvist, 1995) and paleoimmunological criteria (detection and characterization of fossil albumin with monoclonal antibodies (Borja *et al.*, 1992). In addition to the scarce fossil remains, other lines of evidence also point toward the presence of hominids in southeastern Spain, e.g. lithic industries and other signs of anthropic activity such as characteristic breakage patterns in long bones, and cut-marks (Gibert & Jiménez, 1991).

The uniqueness and importance of these paleoanthropological findings necessitate the use of highly accurate techniques to ensure the correct systematic attribution of these fossils. The present article reports our application of different morphometric methodologies, and multivariate analysis, in a comparative analysis of CV-0 with human, pongid and cercopithecid phalanges. The conceptual basis of this work consists in the discrimination of the above mentioned taxa in terms of phalangeal morphology and, especially, of the unequal development of diaphyseal cortex, which is related to the different functions of the hand in these genera (strictly prehensile in humans, prehensile and ambling in pongids, prehensile and running in cercopithecids), and is reflected in the detailed anatomy of the second phalanges. Without any doubt it would be better to analyse phalanges of *Theropithecus*, but we could not find any published measurement or radiograph, and this genus was not present in the collections in the museums and zoological gardens available to our study. However, there can only be small anatomical differences between the second phalanges in *Theropithecus* and the large cercopithecids studied here (*Papio* and *Mandrillus*), given that the life habits of *Theropithecus* were close to those of *Papio*, and the functions of the hand are therefore very similar in both cases.

Analysis with Conventional Variates

Figure 2 shows the results of a linear discriminant analysis of human phalanges compared with *Gorilla*

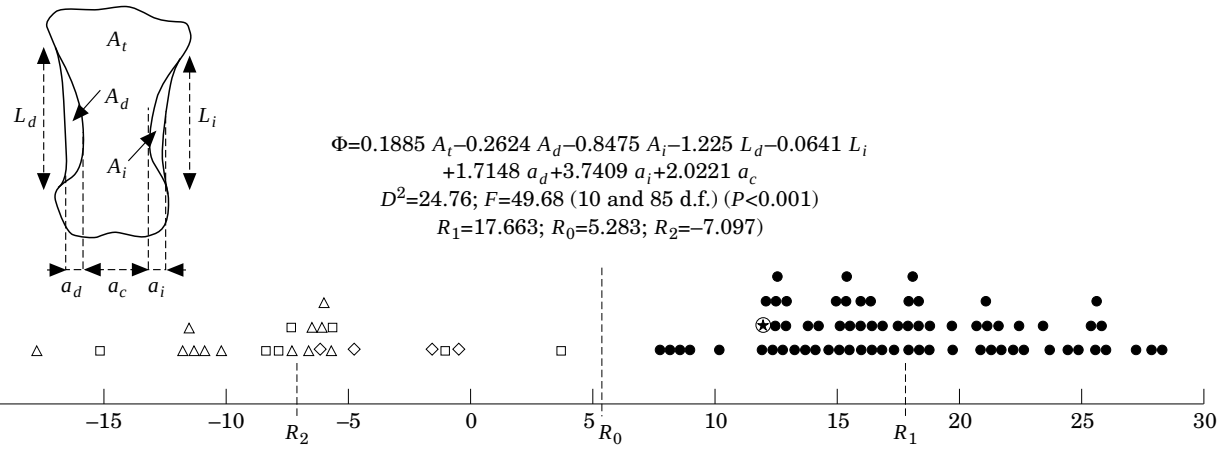

Figure 2. Discriminant analysis between *Homo* and *Gorilla, Papio* and *Mandrillas* phalanges, using conventional variates (distances and surface areas) measured by image analysis on radiographs (data from Santamaría & Gibert, 1992). One hundred per cent of correct reclassifications were obtained. The value obtained for the Cueva Victoria phalanx in the discriminant function places the fossil within the human group. ⍟ = Cueva Victoria; ● = *Homo*; □ = *Gorilla*; ◇ = *Papio*; △ = *Mandrillus*.

gorilla, Papio hamadryas and *Mandrillus sphinx* phalanges. We used as variates conventional parameters (distances and surface areas), which were estimated on radiographs by Santamaría & Gibert (1992). The graph shows that the discriminant function (φ) correctly assigned all specimens analysed to their respective universes, with no overlap between both groups. The Mahalanobis distance between the centroids of each group (D^2=24·76) indicated, on the basis of Hottelling's T-test and its associated F statistic (see Davis, 1986; Reyment *et al*., 1984), that the difference between both multivariate mean values was highly significant (F=46·68, P<0·001). The value obtained for the Cueva Victoria phalanx in the discriminant function clearly showed the fossil to be within the sample of human phalanges.

However, classical variates (e.g. distances, surface areas and angles) have disadvantages that may limit their usefulness as morphometric descriptors of fossils (Scott, 1980; Benson & Chapman, 1982; Palmqvist, 1989; González-Donoso & Palmqvist, 1990; Rohlf & Bookstein, 1990; Bookstein, 1991; Reyment, 1991): they cannot distinguish adequately between morphological features related with size and shape, they do not take into account the relative positions of the homologous points or landmarks in specimens to be compared, and they provide no access to the wealth of information contained in the curvatures of biological outlines—an extremely important feature for the visual recognition of morphological differences. Moreover, most biometric studies that have used these variates were not designed on the basis of any pre-existing theoretical framework (e.g. with regard to what exactly it was necessary to measure), but simply attempt to take as many measurements as possible. The problem with this approach is that the variates are redundant in many cases, i.e. are partly or completely subsumed within one another. This affects the outcome of multivariate analyses, as there exists a priori a certain degree of correlation between the variates. For these reasons, the present study was designed to contrast the results of the classical morphometric approach explained above with those obtained using other more advanced methodologies for shape analysis.

Analysis of Outlines

Several methods have been developed to analyse the shape and curvature of biological outlines, including the different modalities of Fourier series analysis (e.g. open or closed outlines, polar radii, elliptic analysis, etc. (for a review see Rohlf, 1990)), eigenshape analysis (Lohmann, 1983; Lohmann & Schweitzer, 1990) and methods to obtain median axes or line skeletons (Straney, 1990). In the present study we used Fourier analysis of closed outlines, following the polar radii approach (Ehrlich & Weinberg, 1970; Palmqvist, 1989), which is perhaps the most widely used technique in morphometrics (see González-Donoso & Palmqvist (1990) and the references in their article).

Fourier series for closed outlines consist of trigonometric equations incorporating sines and cosines, which can be used to describe and reproduce, as precisely as needed, any bidimensional figure, provided that any radius departing from its centre of gravity intercepts only the periphery of the outline once. The shape outline is estimated from the following equation, which adjusts the expansion of a radius running from the centre of gravity of the outline to its periphery, as a function of the rotation angle (θ) in a polar coordinate system whose origin is located in the centroid. The radius (R,θ) is given by:

$$R(\theta) = R_0 [1 + \sum_{n=1}^{\alpha} A_n \cos(n\theta) + \sum_{n=1}^{\alpha} B_n \sin(n\theta)],$$

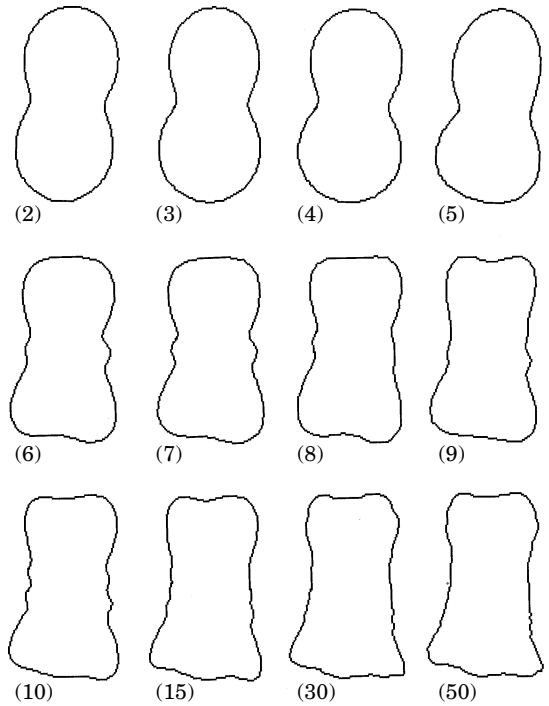

Figure 3. Computer-generated graphical simulations of the Cueva Victoria phalanx outline obtained using Fourier analysis of polar radii. Numbers refer to the harmonic order used for each simulation.

an equation that is normally used in the following transformation:

$$R(\theta) = R_0 [1 + \sum_{n=1}^{\alpha} C_n \cos(n\theta - P_n)],$$

$$\text{with } C_n = (A_n^2 + B_n^2)^{1/2} \text{ and } P_n = \arctan (B_n/A_n),$$

where θ is the polar angle formed by the radius $R(\theta)$ with a horizontal reference line that crosses the centre of masses of the outline, R_o is the radius of a circumference with equivalent area to that of the specimen being analysed, n is the harmonic order number, C_n is the harmonic amplitude of the nth-order harmonic and P_n is its phase angle (see Appendix 1 for the adjustment of these equations).

The precision of Fourier analysis in characterizing an outline depends on the number of coordinates initially taken to determine its periphery and on the number of harmonics used in the adjustment of the series. As a rule, at least twice the number of peripheral points must be estimated as the number of the highest harmonic desired. This analysis allows the specimen to be split into its geometrical components, regardless of its size and without the necessity of having homologous points. The characterization of the outline may be as accurate as desired (see Figure 3). Particularly, the amplitudes of low order harmonics estimate the global geometric aspects of the analysed outline, while amplitudes of higher order harmonics consider aspects of increasingly fine-scaled sculpture. Thus, it may be considered that the amplitude of the second harmonic represents the contribution to the empirical shape of a figure eight, and is thus a measure of the elongation of the outline. The third harmonic estimates the contribution of a trefoil, a measure of its triangularity. In general, the nth-order harmonic amplitude represents the shape contribution of a n-leaved clover. The amplitude of the first harmonic is a measure of the error produced in the adjustment of the Fourier series to the outline. Phase angles, divided by their corresponding harmonic order, indicate in which place of the figure the influence of harmonics is located. These parameters may be employed as multivariate shape descriptors (Younker & Ehrlich, 1977).

Any proposed system of shape analysis will be considered in a different manner by its detractors and its defenders. Fourier analysis of closed outlines presents some theoretical limitations and possible disadvantages from a practical standpoint (Bookstein *et al.*, 1982; Lohmann, 1983; Ehrlich, Pharr & Healy-Williams, 1983; Rohlf, 1990): (1) Fourier series of polar radii are only useful in expanding single valued functions, (2) the centroid of the outline (to which all radii will be referred) cannot be considered a homologous point between two analysed specimens, and (3) while the shape of an outline can be completely represented by its Fourier transform, it is more difficult in certain cases (except for the lowest order harmonics) to know how the individual terms of the Fourier series reflect the different morphological features in the original shape. As a consequence of this, the relationship between a shape and its harmonic function is not simple, except for periodic or radially symmetric forms (like those typified, for example, by the exoskeleton of echinoderms), but not for the more common aperiodic outlines.

Elliptic Fourier analyses (Kuhl & Giardina, 1982; Rohlf & Archie, 1984; Rohlf, 1990) allows us to analyse those complex and intricate closed contours, where a radius departing from the centre of gravity intercepts the periphery more than once. This method is based on the separate Fourier decompositions of the first differences of the x and y coordinates as parametric functions of the cumulative chordal distance of the points around the outline. Two coefficients are estimated for both the x and y-projections, and thus four parameters (A_n, B_n, C_n and D_n) are used for each harmonic. Given the smooth outline of the analysed phalanges, which were single-valued for polar radii from the centroid in all specimens, were discarded the elliptic approach because it required a greater number of variates to characterize the phalanges.

Figure 3 illustrates several computerized simulations of the contour of the Cueva Victoria phalanx, which were obtained by incorporating successive harmonics into the Fourier series fitted to the original outline. These simulations show that the first harmonics describe the overall geometric components of the shape

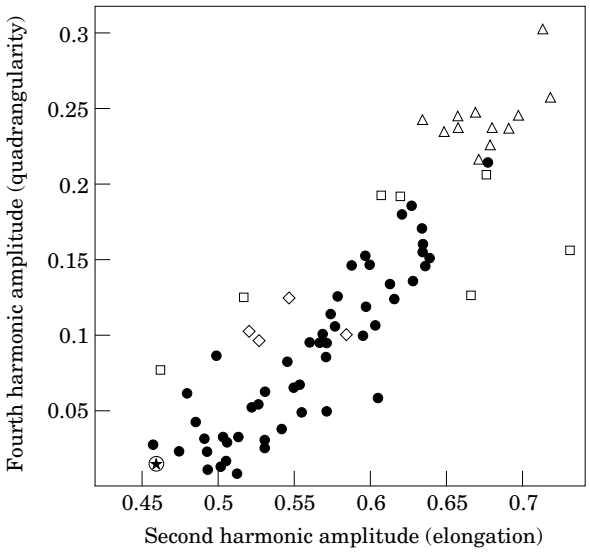

Figure 4. Bivariate plot of amplitude values for the second and fourth harmonics of the Fourier series in human, gorilla and cercopithecid phalanges. Note the location of the Cueva Victoria phalanx within the region of morphospace occupied exclusively by hominids. ⊛ = Cueva Victoria; ● = *Homo*; □ = *Gorilla*; ◇ = *Papio*; △ = *Mandrillus*.

(e.g. the elongation, triangularity, quadrangularity, etc. of the specimen), whereas reproduction of more localized details requires a greater number of terms in the harmonic series. Although a relatively large number of harmonics (30–50) were necessary to thoroughly characterize and reproduce the outline, its major features are adequately described with the first 10 harmonics. We therefore only used these as variates in the multivariate analyses.

Figure 4 shows that human phalanges were distinguishable to a certain degree from gorilla and cercopithecid ones by considering only the second and fourth harmonic amplitudes, which estimate the elongation and quadrangularity of the outlines, respectively. The fossil phalanx was located in the region of the bivariate plot occupied exclusively by hominids.

To obtain an overall estimation of these differences from a multivariate perspective, we repeated the discriminant analysis using a new set of variates. The harmonic amplitudes of the first 10 harmonics (except for the first term of the series, which measures only errors of adjustment) were considered as shape descriptors, and the surface area of the phalanges was used as a size estimator. The results (Figure 5) showed that the form of the phalanx outline (multivariate means) in the two compared groups (humans versus gorillas and cercopithecids) differed significantly ($D^2 = 16{\cdot}06$; $F = 22{\cdot}10$; $P < 0{\cdot}001$), although the extremes of both distributions overlapped slightly (96% correct reassignments with the discriminant function). Nevertheless, the value obtained for the Cueva Victoria in the discriminant function placed the fossil in the human group, near its centroid.

Landmark Analyses

The relative positions of landmarks was analysed with three methodologies from Geometric Morphometry (Bookstein *et al.*, 1985; Bookstein, 1991; Reyment, 1991): estimation of shape coordinates, principal and relative warp analyses. The first method is based on the following premises: for a set of N landmarks with their corresponding cartesian coordinates (x,y), a total of N-2 triangles can be constructed. In each triangle the original coordinates of the landmarks can be transformed such that the first and second serve as a reference baseline, with values of (0,0) and (1,0). The shape of the triangle is then defined by the new coordinates (x',y') for the third point (see Figure 6, which also gives the algorithms needed for the transformation).

The conceptual basis of principal warp analysis is as follows (Bookstein, 1989; 1991): any change between two specimens that affects the two-dimensional

$\Phi = 0.013\,S + 3.935\,C_2 + 114.597\,C_3 - 53.767\,C_4 + 159.709\,C_5 + 142.946\,C_6 + 18.936\,C_7$
$- 12.621\,C_8 - 132.532\,C_9 + 120.153\,C_{10}$
$D^2 = 16.06$; $F = 22.099$ (10 and 63 d.f.) ($P < 0.001$);
$R_1 = 13.886$; $R_0 = 21.918$; $R_2 = 29.95$

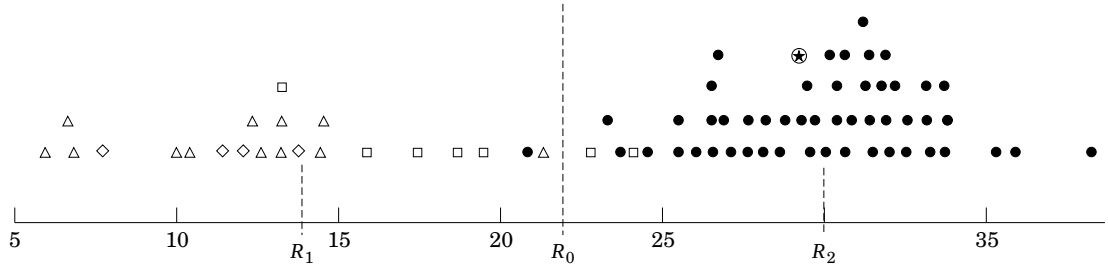

Figure 5. Discriminant analysis of the outline of human phalanges in comparison with gorilla and cercopithecid phalanges, using the harmonic amplitudes (C_2–C_{10}) of the Fourier series, and surface area (S) enclosed within the outline. The function yielded 95·9% correct assignments and placed the Cueva Victoria phalanx within the human group. ⊛ = Cueva Victoria; ● = *Homo*; □ = *Gorilla*; ◇ = *Papio*; △ = *Mandrillus*.

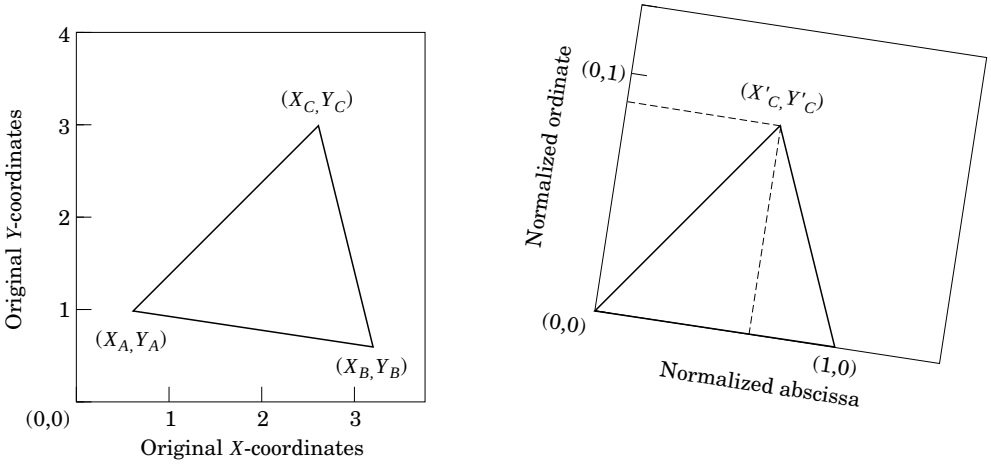

$$X'_C=[(X_B-X_A)(X_C-X_A)+(Y_B-Y_A)(Y_C-Y_A)]/[(X_B-X_A)^2+(Y_B-Y_A)^2]$$
$$Y'_C=[(X_B-X_A)(Y_C-Y_A)-(Y_B-Y_A)(X_C-X_A)]/[(X_B-X_A)^2+(Y_B-Y_A)^2]$$

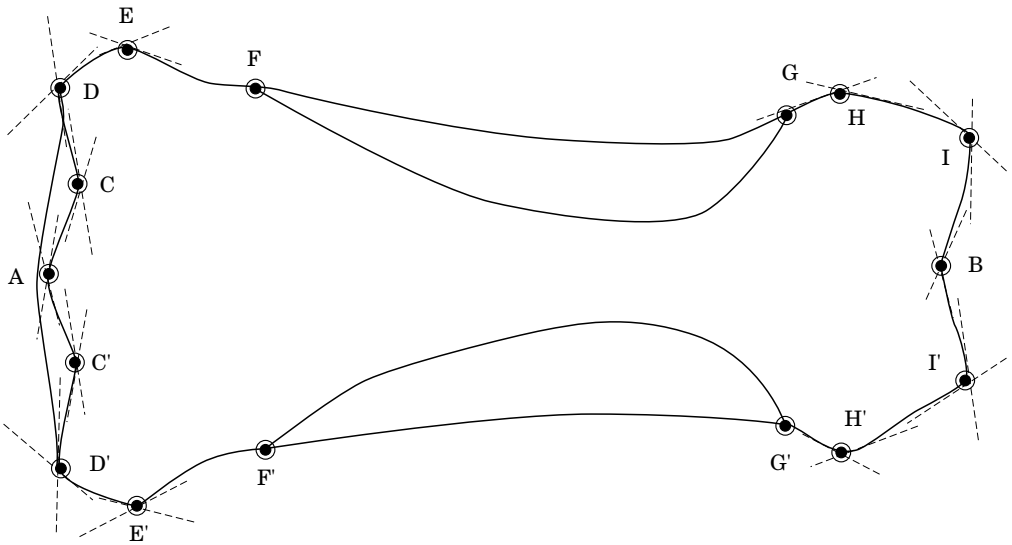

Figure 6. Calculation of shape coordinates for triangles of landmarks (redrawn after Figure 5.1.2 in Bookstein, 1991), and selected landmarks on radiographs of the phalanges. See the text for an explanation of the method.

configuration of a set of landmarks, in terms of their relative positions in both specimens, can be expressed (and characterized morphometrically) by means of a uniform (or affine) transformation and a non-uniform (or non-affine) component. The affine part can be interpreted as a series of changes in scale along bi-orthogonal axes, giving rise to an anisotropy measure (e.g. dilation in one direction and contraction in the orthogonal one). This type of transformation leaves parallel lines unchanged, and displaces the landmarks in a manner proportional to their original distances from the reference baseline, without bending the cartesian plane the lines lie in. Thus, the bending energy to be transferred to the plane is null. The non-uniform part of the change in position of the landmarks involves deformations of the plane they lie in, giving rise to local bending. This bending can be expressed as a sum of the partial warps that represent the regional components of the change in the positions of landmarks, and that can be calculated as eigenvectors of the total bending energy, once the affine variation has been removed. It should be noted that the greatest

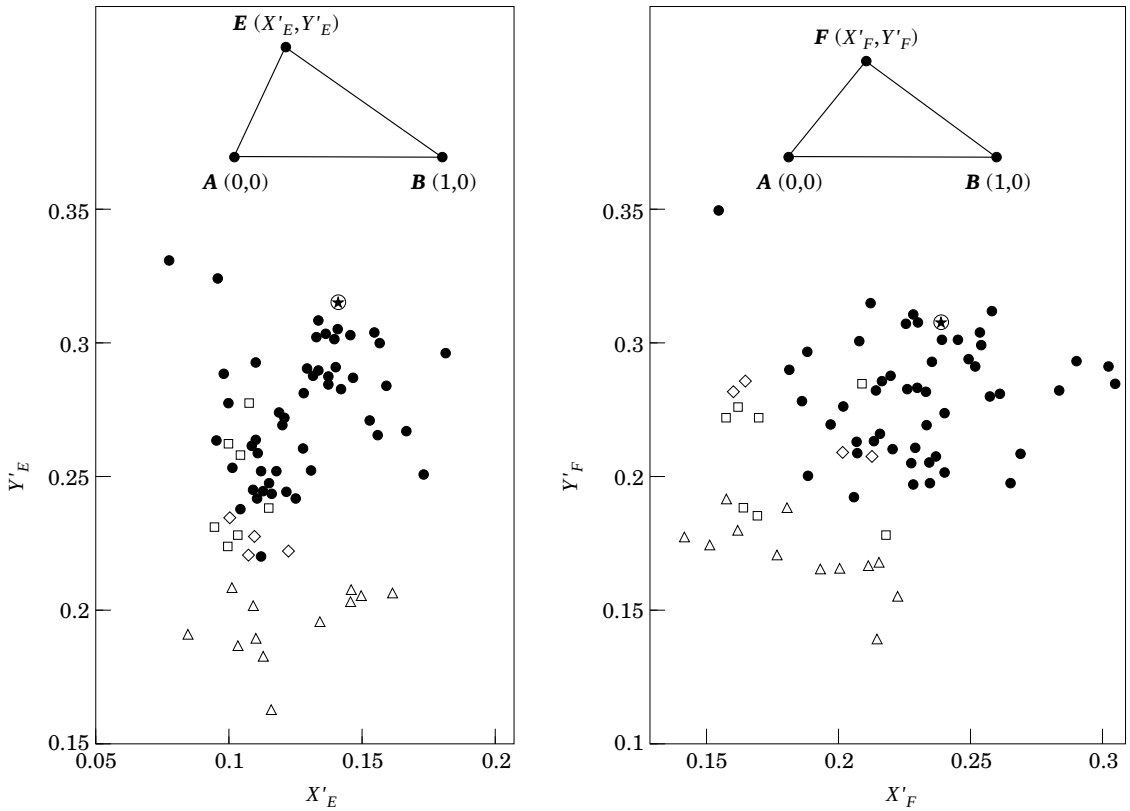

Figure 7. Values obtained for the shape coordinates of triangles formed by landmarks ***AEB*** and ***AFB*** on the phalanges analysed; the baseline was defined by points ***A*** and ***B***. Note that in both graphs, the Cueva Victoria phalanx is located within the morphospatial regions occupied exclusively by human phalanges. ⊛ = Cueva Victoria; ● = *Homo*; □ = *Gorilla*; ◇ = *Papio*; △ = *Mandrillus*.

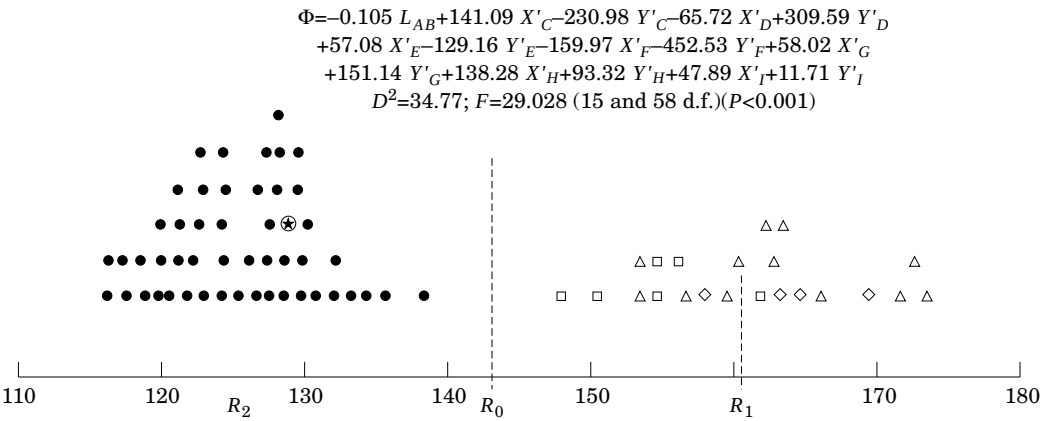

Figure 8. Discriminant analysis of human phalanges compared with gorilla and cercopithecid phalanges, using shape coordinates (X', Y') of landmarks ***C, D, E, F, G, H*** and ***I***, and baseline ***AB*** length as variates. The function yielded 100% correct reclassifications, and assigned the Cueva Victoria phalanx to the human group. ⊛ = Cueva Victoria; ● = *Homo*; □ = *Gorilla*; ◇ = *Papio*; △ = *Mandrillus*.

energy is given by the partial warps that describe the most localized deformations, affecting the positions of nearby landmarks; these warps thus have lower eigenvalues. In contrast, more general changes are associated with those components which have the greatest eigenvalues, and thus require lower bending energies.

The mathematical details of these methodologies, and a number of paleobiological applications, are given in Bookstein (1989; 1991), Rohlf & Bookstein (1990), Reyment (1991; 1993), Rohlf (1993), Reyment & Jöreskog (1993), O'Higgins & Dryden (1993), and Marcus, Bello & García-Valdecasas (1993). The diagrams shown in this article (Figures 9–11) were

prepared from results obtained from the TPSPLINE and TPSRW software developed by Rohlf (in Rohlf & Bookstein, 1990; Marcus *et al.*, 1993) (see Appendix 2 for mathematical details).

Selected landmarks on the phalanges are shown in Figure 6. Points ***A, B, C, D, E, H*** and ***I*** can be considered type II landmarks (*sensu* Bookstein, 1991), as they correspond to regions of the phalanx outline with marked local change in curvature. Their position can be estimated from the point where two tangential lines intersect the outline. Points ***F*** and ***G***, in contrast, are type I landmarks, given their more precise anatomical definition at points where the cortical intersects the outline of the phalanx. Landmarks ***A*** and ***B*** were used to establish the baseline, with reference to which we estimated the shape coordinates of the remaining points. For each landmark except ***A*** and ***B***, we estimated its position on both sides of the phalanx (e.g. ***C*** and ***C′*** in Figure 6), and then averaged its shape coordinates so that the results of subsequent analyses would be equally applicable to right or left phalanges.

Figure 7 shows the results obtained for triangles formed by landmarks ***ABE*** and ***ABF***. Some degree of separation was obtained for the shape coordinates (X', Y') of points ***E*** and ***F***, between the values estimated for humans and other primates in the analysis. Interestingly, in both cases, the Cueva Victoria phalanx was situated in the region of the morphospace occupied exclusively by hominids. The discriminant function that includes as variates all landmarks and baseline length is shown in Figure 8. Both groups show no overlapping in the function, the multivariate means are significantly different ($D^2 = 34{\cdot}77$; $F = 29{\cdot}03$; $P < 0{\cdot}001$), and there was 100% correct reclassification. When the discriminant function was applied to the fossil phalanx, the resulting value placed it, once again, clearly within the human group.

The results of principal warp analysis are shown in Figure 9, which illustrates the transformation diagrams required to change the relative position of landmarks in the Cueva Victoria phalanx to the mean locations of landmarks for *Homo, Gorilla, Papio* and *Mandrillus* phalanges, respectively. To remove the effects of the original size of the phalanges and concentrate exclusively on their shape, mean configurations of landmarks both in the fossil and in the groups for comparison were calculated on the basis of unit length for baseline ***AB***.

Warp diagrams show the uniform and non-uniform variation together. To facilitate comparisons, the bending energy required to align the landmarks of the Cueva Victoria phalanx with those of each reference mean phalanx in the Cartesian plane are given. We should note that this parameter is not the best metric to characterize changes in landmark configuration, as it does not distinguish between the different local components of bending (which are described by the partial warps), but rather treats them as a single entity. However, in the case at hand, the analyses provide a general indication of the whole differences between the relative positions occupied by the fossil phalanx landmarks and those on each reference group. Thus, the warp diagram for *Homo* has a low bending energy (0·00797), similar or even lower than that value needed to transform a given human phalanx into one defined by the mean landmark positions for the entire group. In contrast, the bending energy value required for transformation into the *Gorilla* phalanx (0·05747) was more than seven-fold higher, because of the greater dilation, contraction and curving required to shift the landmarks in different regions of the Cartesian plane (see Figure 9). Bending energies in the diagrams for *Mandrillus* (0·06458) and *Papio* (0·17461) were even higher than those noted above, reflecting that the

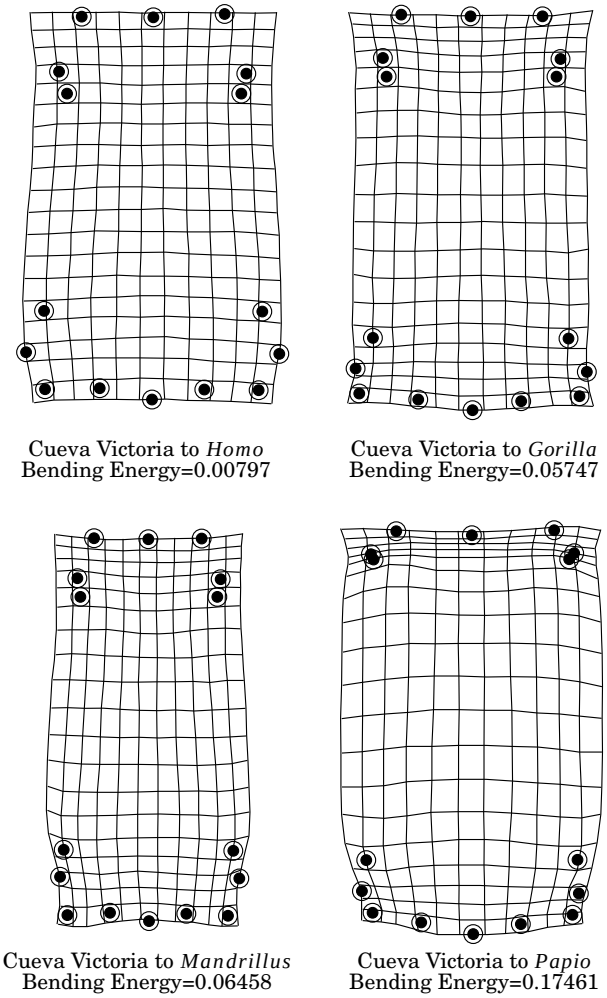

Figure 9. Comparison with principal warp analysis between the positions of landmarks on the Cueva Victoria phalanx and mean configurations of landmarks on human, gorilla and cercopithecid phalanges. The points represent those landmarks used in the analysis (see Figure 6). The graphs were generated using the TPSPLINE software developed by Rohlf (in Rohlf & Bookstein, 1990; Marcus *et al.*, 1993). Warp diagrams show affine or uniform and non-uniform variation together, and bending energy values associated with each transformation are given.

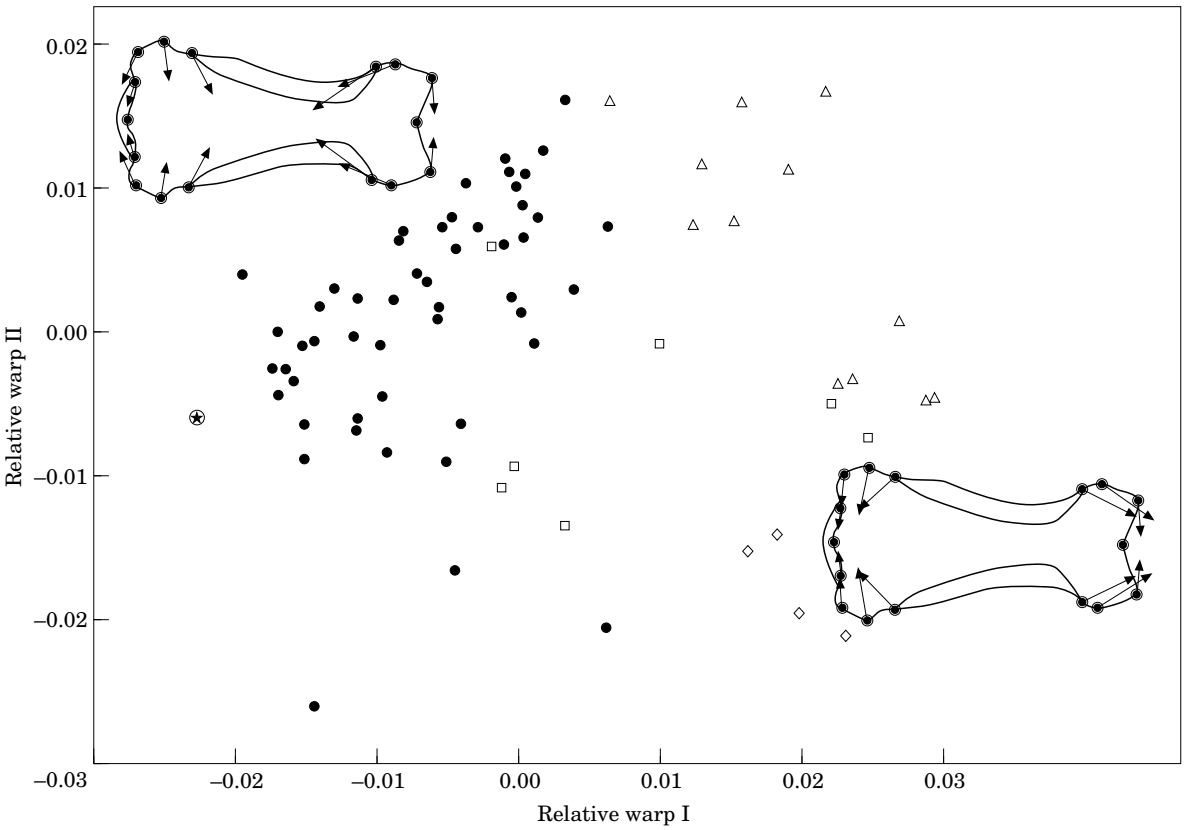

Figure 10. Bivariate plot of relative warps I and II for landmarks ***A–I*** in Cueva Victoria, human, gorilla and cercopithecid phalanges. The calculations were performed with TPSRW software developed by Rohlf (in Marcus *et al*., 1993), and using $\alpha=0$. The arrows show vector displacements of landmarks along relative warps. ⊛ = Cueva Victoria; ● = *Homo*; □ = *Gorilla*; ◇ = *Papio*; △ = *Mandrillus*.

relative positions of landmarks in these two mean phalanges differed more markedly from those of the Cueva Victoria specimen.

The method of relative warps (Bookstein, 1989; 1991; Rohlf, 1993) analyses the variation within a sample as the variance in the parameters of interpolating fitted functions (thin-plate splines) between the positions of landmarks in each specimen and those occupied in a reference configuration; usually, this latter is the mean location of landmarks in the sample after the objects have been aligned according to a reasonable criterion (e.g. with reference to a baseline). The relative warps are then computed as eigenvectors of a matrix with its rows corresponding to the specimens and the columns corresponding to their scores in the principal warps, which have been scaled to a power (α) of their eigenvalues. Thus, the relative warps can be considered as the vectors of principal components which explain the variance in shape among the individuals due to non-uniform transformations.

Although the relative warps method was originally developed to describe the variation in locations of landmarks in a set of objects related to non-affine transformations between the consensus configuration and each specimen within a sample (Bookstein, 1991), posterior statistical modifications have been introduced by Rohlf (1993) and they allow us to analyse, jointly with the non-uniform changes, the affine part that is orthogonal to the principal warps, if the warps that explain large-scale features are not weighted in relation to the principal warps corresponding to small-scale features ($\alpha=0$). This variant of the method has been applied in the present work to the shape coordinates of specimen landmarks, which were superimposed based on the minimum energy criterion.

The scatterplots of the scores of each phalanx on the relative warp II and III axes versus relative warp I axis are shown in Figures 10 and 11, respectively. It can be seen that the Cueva Victoria phalanx is placed, in both cases, in the regions dominated by *Homo*. Furthermore, on each axis the respective relative warp loadings have been drawn as displacement vectors at each landmark on the reference configuration, pointing in those directions of maximum variance in the locations of landmarks that are explained by each relative warp. The major variation within *Homo* specimens is located along the third relative warp, whereas among *Mandrillus, Papio* and *Gorilla*, it occurs among the second one. The different arrangement of *Homo* and Cueva Victoria phalanges with regard to those of other analysed genera is manifested along the first relative warp. This warp is related to a contraction in a transverse

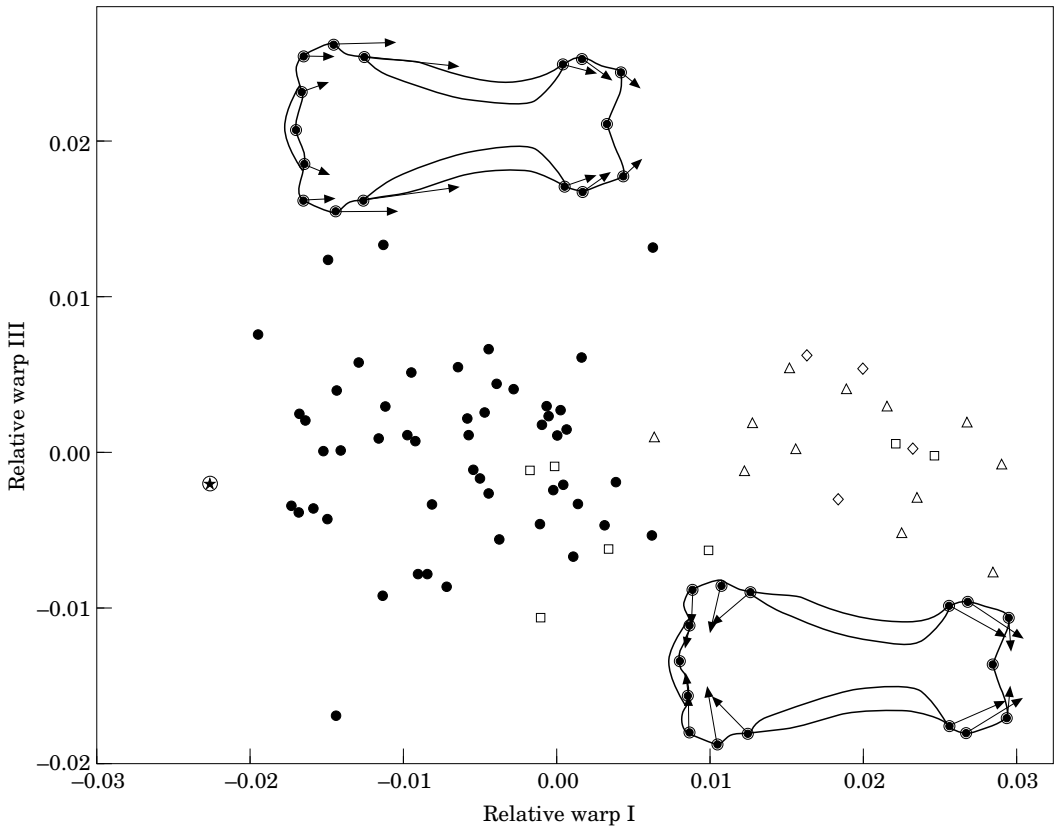

Figure 11. Bivariate plot of relative warps I and III for landmarks ***A–I*** in Cueva Victoria, human, gorilla and cercopithecid phalanges. The calculations were performed with TPSRW software developed by Rohlf (in Marcus *et al.*, 1993), and using $\alpha=0$. The arrows show vector displacements of landmarks along relative warps.

direction of landmarks placed on the proximal region of the phalanx, jointly with a longitudinal dilation of those landmarks placed on the distal end of the phalanx.

The results of principal and relative warp analysis thus fully concur with those provided by other morphometric analyses used in this study, and provide clear evidence of the human affinity of the fossil.

Conclusions

The morphometric analyses with conventional variates, Fourier series, shape coordinates of landmarks, principal and relative warps, strongly suggest that the Cueva Victoria phalanx differs markedly from pongid and cercopithecid phalanges, and is from a member of the genus *Homo*. The presence of *Homo* in the south of the Iberian Peninsula during the Lower Pleistocene is a finding that can potentially shed light on human dispersal from Africa, a migration that has thus far been believed to have had only one destination, eastern Asia.

Acknowledgements

This study was supported by a Spanish governmental major research grant, Project PB94-1222, from the Dirección General Interministerial de Ciencia y Tecnología. We thank Ms. Karen Shashok for translating the original manuscript into English. We gratefully acknowledge constructive remarks made by two anonymous reviewers.

References

Benson, R. H. & Chapman, R. E. (1982). On the measurement of morphology and its change. *Paleobiology* **9,** 398–413.

Bookstein, F. L. (1991). *Morphometric Tools for Landmark Data*. New York, NY: Cambridge University Press.

Bookstein, F. L. (1989). Principal warps: thin-plate splines and the decomposition of deformations. *IEEE Transactions on Pattern Analysis and Machine Intelligence* **11,** 567–585.

Bookstein, F. L., Strauss, R. E., Humphries, J. M., Chernoff, B., Elder, R. L. & Smith, G. R. (1982). A comment upon the uses of Fourier methods in Systematics. *Systematic Zoology* **31,** 85–92.

Bookstein, F. L., Chernoff, B., Elder, R. L., Humphries, J. M., Smith, G. R. & Strauss, R. E. (1985). *Morphometric in Evolutionary Biology. The Geometry of Size and Shape Change, with Examples from Fishes*. Philadelphia: The Academy of Natural Sciences of Philadelphia, PH: Special Publication No 15.

Borja, C., García-Pacheco, J. M., Ramírez-López, J. P. & García-Olivares, E. (1992). Cuantificación y caracterización de la albúmina fósil de cráneo de Orce. In (J. Gibert, Coord.) *Proyecto Orce-Cueva Victoria (1988–1992), Presencia humana en el Pleistoceno inferior de Granada y Murcia*. Granada: Ayuntamiento de Orce, pp. 415–423.

Davis, J. (1986). *Statistics and Data Analysis in Geology*. 2nd edition. New York, NY: John Wiley & Sons.

Ehrlich, R. & Weinberg, B. (1970). An exact method for characterization of grain shape. *Journal of Sedimentary Petrology* **40,** 205–212.

Ehrlich, R., Pharr, B. & Healy-Williams, N. (1983). Comments on the validity of Fourier descriptors in Systematics: a reply to Bookstein *et al. Systematic Zoology* **32,** 202–206.

Ferrández, C., Pérez-Cuadrado, J. L., Gibert, J. & Martínez-Navarro, B. (1989). Estudio preliminar de los sedimentos de relleno de Cueva Victoria (Catagena, Murcia). In (J. Gibert, D. Campillo & E. García-Olivares, Eds.) *Los Restos Humanos de Orce y Cueva Victoria*. Sabadell: Institut Paleontológic "Dr. M. Crusafont", pp. 379–394.

Gibert, J. & Pons, J. (1984). Estudio morfológico de la falange del género *Homo* de Cueva Victoria (Cartagena, Murcia). *Paleontología y Evolució* **XVIII,** 49–56.

Gibert, J. & Pérez, A. (1989). A human phalanx from the Lower Palaeolithic site of Cueva Victoria (Murcia, Spain). *Human Evolution* **4,** 307–316.

Gibert, J. & Jiménez, C. (1991). Investigations into cut-marks on fossil bones of Lower Pleistocene age from Venta Micena (Orce, Granada, Spain). *Human Evolution* **6,** 117–128.

Gibert, J. & Palmqvist, P. (1995). Fractal analysis of the Orce skull sutures. *Journal of Human Evolution* **28,** 561–575.

Gibert, J., Pons, J. & Ruz, M. C. (1985). Comparación métrica y morfológica de la falange del género *Homo* de Cueva Victoria (Cartagena, Murcia) con las de primates y úrsidos. *Paleontología i Evolució* **XIX,** 147–154.

Gibert, J., Campillo, D., Caporicci, R., Ribot, F., Ferrández, C. & Martinez, B. (1989). Anatomical study: comparison of the hominid cranial fragment from Venta Micena Corce, Spain) with fossil and extant mammals. *Human Evolution* **4,** 283–305.

Gibert, J., Leakey, M., Ribot, F., Arribas, A., Martínez-Navarro, B. & Gibert, L. (1995). Presence of the cercopithecid genus *Theropithecus* in Cueva Victoria (Murcia, Spain). *Journal of Human Evolution* **28,** 487–493.

Gibert, J., Sánchez, F., Malgosa, A., Walker, M. J., Palmqvist, P., Martínez-Navarro, B. & Ribot, F. (1992). Nuevos descubrimientos de restos humanos en los yacimientos de Orce y Cueva Victoria. In (J. Gibert, Coord.) *Proyecto Orce-Cueva* Victoria (1988–1992), *Presencia Humana en el Pleistoceno Inferior de Granada y Murcia.* Granada: Ayuntamiento de Orce, pp. 391–413.

González-Donoso, J. M. & Palmqvist, P. (1990). Sobre la caracterización biométrica del crecimiento y la forma de los foraminíferos planctónicos. Aplicación de las series de Fourier al análisis de la forma de las cámaras. *Revista Española de Paleontología* **5,** 81–90.

Kuhl, F. P. & Giardina, C. R. (1982). Elliptic Fourier features of a closed contour. *Computer Graphics and Image Processing* **18,** 236–258.

Lohmann, G. P. (1983). Eigenshape analysis of microfossils: a general morphometric procedure for describing changes in shape. *Mathematical Geology* **15,** 659–672.

Lohmann, G. P. & Schweitzer, P. N. (1990). On eigenshape analysis. In (F. J. Rohlf & F. L. Bookstein, Eds) *Proceedings of the Michigan Morphometrics Workshop*. The University of Michigan Museum of Zoology, Special Publication No 2, pp. 147–166.

Marcus, L. F., Bello, E. & García-Valdecasas, A. (1993). *Contributions to Morphometrics*. Madrid: Monografías del Museo Nacional de Ciencias Naturales de Madrid (C.S.I.C), **8**.

Musgrave, J. H. (1969). A comparative study of the hand bones of the Neanderthal man. *Human Biology* **41,** 587–588.

Musgrave, J. H. (1971). How dextrous was Neanderthal man? *Nature* **233,** 538–541.

O'Higgins, P. & Dryden, I. L. (1993). Sexual dimorphism in hominoids: further studies of craniofacial shape differences in *Pan, Gorilla* and *Pongo. Journal of Human Evolution* **24,** 183–205.

Palmqvist, P. (1989). *Análisis del crecimiento y la forma en los foraminíferos planctónicos, con fines biométricos*. Ph. D. Thesis, University of Málaga (Spain).

Pons Moyá, J. (1985). Nota preliminar sobre el hallazgo de *Homo* sp. en los rellenos cársticos de Cueva Victoria (Murcia, España). *Endins* **10–11,** 47–50.

Reyment, R. A. (1991). *Multidimensional Palaeobiology*. Oxford: Pergamon Press.

Reyment, R. A. (1993). Ornamental and shape variation in *Hemicytherura fulva* McKenzie, Reyment and Reyment (Ostracoda; Eocene, Australia). *Revista Española de Paleontología* **8,** 125–131.

Reyment, R. A. & Jöreskog, K. G. (1993). *Applied Factor Analysis in the Natural Sciences*. 2nd Edition, Cambridge: Cambridge University Press.

Reyment, R. A., Blackith, R. E. & Campbell, N. A. (1984). *Multivariate Morphometrics*. 2nd Edition. London: Academic Press.

Rohlf, F. J. (1990). Fitting curves to outlines. In (F. J. Rohlf & F. L. Bookstein, Eds.) *Proceedings of the Michigan Morphometrics Workshop*. The University of Michigan Museum of Zoology, Special Publication No 2, pp. 167–177.

Rohlf, F. J. (1993). Relative warp analysis and an example of its application to mosquito wings. In (L. F. Marcus, E. Bello & A. García-Valdecasas, Eds.) *Contributions to Morphometrics*. Madrid: Museo Nacional de Ciencias Naturales, pp. 131–159.

Rohlf, F. J. & Archie, J. (1984). A comparison of Fourier methods for the description of wing shape in mosquitoes (*Diptera: Culicidae*). *Systematic Zoology* **33,** 302–317.

Rohlf, F. J. & Bookstein, F. L. (Eds) (1990). *Proceedings of the Michigan Morphometrics Workshop*. The University of Michigan Museum of Zoology, Special Publication No 2.

Santamaría, J. L. & Gibert, J. (1992). Comparación métrica radiológica de la falange de *Homo* sp. de Cueva Victoria (Cartagena, Murcia) y otros primates. In (J. Gibert, Coord.) *Proyecto Orce-Cueva Victoria (1988–1992), Presencia Humana en el Pleistoceno Inferior de Granada y Murcia*. Granada: Ayuntamiento de Orce, pp. 431–444.

Scott, G. H. (1980). The value of outline processing in the biometry and systematics of fossils. *Palaeontology* **23,** 757–768.

Straney, D. O. (1990). Median axis methods in morphometrics. In (F. J. Rohlf & F. L. Bookstein, Eds.) *Proceedings of the Michigan Morphometrics Workshop*. The University of Michigan Museum of Zoology, Special Publication No 2, pp. 179–200.

Younker, J. L. & Ehrlich, R. (1977). Fourier biometrics: harmonic amplitudes as multivariate shape descriptors. *Systematic Zoology* **26,** 336–342.

APPENDIX 1: Adjustment of Fourier series for closed outlines: mathematical details; from Palmqvist (1989)

The basic equation of Fourier analysis, which describes the expansion of a radius [$R(\theta)$] running from the centre of gravity of the outline to its periphery, as a function of the rotation angle (θ) in a polar coordinate system whose origin is located in the centroid of the figure,

$$R(\theta) = R_0 [1 + \sum_{n=1}^{\alpha} A_n \cos(n\theta) + \sum_{n=1}^{\alpha} B_n \sin(n\theta)],$$

may be easily fitted to a given outline by the following steps:

(1) A set (100–500) of cartesian coordinates of points describing the periphery of the projection of each phalanx are taken with a digitizer tablet. The number of points depends on the degree of precision required in the ensuing analysis. The coordinate locations on the outline are arbitrary but, as a general rule, more coordinates are needed in those parts of the outline with the most abrupt changes of curvature, while less points will suffice to define smooth regions. Coordinates must be consecutively taken in a clockwise

rotation. If we wish to retain the information relative to the orientation of harmonics in the outlines, only two equivalent points are needed to rotate all figures to the same position. When we have calculated the (x,y) coordinates of L points the outline is closed by assuming $X_{L+1}=X_1$ and $Y_{L+1}=Y_1$.

(2) The next step is to calculate the area of the outline, using the following equation:

$$A=\sum_{j=1}^{L}[(Y_{j+1}+Y_j)(X_j-X_{j+1})]/2,$$

(3) Then, the first total moments about the X-axis and the Y-axis are estimated:

$$My=\sum_{j=1}^{L}[(Y_{j+1}^2+Y_{j+1}Y_j+Y_j^2)(X_j-X_{j+1})]/6,$$

$$Mx=\sum_{j=1}^{L}[(X_{j+1}^2+X_{j+1}X_j+X_j^2)(Y_j-Y_{j+1})]/6,$$

and the cartesian coordinates of the centroid are given by dividing the appropriate total moments by the area of the outline:

$$X_c=MX/A \text{ and } Y_c=MY/A.$$

(4) Each of the initial L points taken along the periphery of the outline may then be expressed in polar coordinates (R,θ) about the centre of gravity as:

$$R_j=[(Y_j-Y_c)^2+(X_j-X_c)^2]^{1/2}$$

$$\theta_j=\arctan[(Y_j-Y_c)/(X_j-X_c)]$$

and again considering that $R_{L+1}=R_1$ and $\theta_{L+1}=\theta_1$.

(5) The next step is to calculate the medium radii of the specimen (R_o), by means of the following equation:

$$R_o=\pi/4\sum_{j=1}^{L}[(R_{j+1}+R_j)(\theta_{j+1}-\theta_j)]/6,$$

in which we note that if θ_{j+1} is located in the first quadrant (0°–90°) and θ_j in the fourth (270°–360°) we must then add 2π to the difference of angles.

(6) The radii of the points that define the periphery of the object are then divided by the medium radii ($R_j^*=R_j/R_o$), which makes the analysis size independent, and the terms A_n and B_n of the harmonic series are then calculated by:

$$A_n=1/\pi\sum_{j=1}^{L}[((R_{j+1}^*-R_j^*)(\cos(n\theta_{j+1})-\cos(n\theta_j)))/((\theta_{j+1}-\theta_j)n^2)+(R_{j+1}^*\sin(n\theta_{j+1})-R_j^*\sin(n\theta_j))/n],$$

and

$$B_n=1/\pi\sum_{j=1}^{L}[((R_{j+1}^*-R_j^*)(\sin(n\theta_{j+1})-sin(n\theta_j)))/((\theta_{j+1}-\theta_j)n^2)-(R_{j+1}^*\cos(n\theta_{j+1})-R_j^*\cos(n\theta_j))/n].$$

APPENDIX 2: Mathematical aspects of principal warp analysis; from Bookstein (1991)

Let be $Z_1=(X_1,Y_1)$, $Z_2=(X_2,Y_2)$, . . ., $Z_k=(X_k,Y_k)$ the cartesian coordinates of K points taken in the reference specimen and $Z'_1=(X'_1,Y'_1)$, $Z'_2=(X'_2,Y'_2)$, . . ., $Z'_k=(X'_k,Y'_k)$ the corresponding coordinates in the other specimen; the next function is defined as: $U_{ij}=r^2_{ij}\log(r_{ij})$, with $r_{ij}=|Z_i-Z_j|=[(X_i-X_j)^2+(Y_i-Y_j)^2]^{1/2}$ (i.e. the euclidean distance between landmarks i and j in the reference specimen); and the following matrices are formed:

59127eq12

$$\boldsymbol{Q}=\begin{bmatrix}1 & X_1 & Y_1\\ 1 & X_2 & Y_2\\ \cdots & \cdots & \cdots\\ 1 & X_k & Y_k\end{bmatrix}, K\times 3$$

$$\boldsymbol{V}=\begin{bmatrix}X'_1 & X'_2 & \ldots & X'_k\\ Y'_1 & Y'_2 & \ldots & Y'_k\end{bmatrix}, 2\times K$$

$$\boldsymbol{Y}=[\,V\,|\,0\;\;0\;\;0\,]$$

which are then combined to form the matrix:

$$\boldsymbol{L}=\begin{bmatrix}P_k & Q\\ Q^T & O\end{bmatrix}, (K+3)\times(K+3)$$

where $\boldsymbol{Q}^T$ is the transposed of $\boldsymbol{Q}$ and $\boldsymbol{O}$ is a matrix of order 3×3, whose elements are zeros.

The bending energy necessary to change the K points from the positions (X, Y) in the reference figure to the positions (X', Y') which they occupy in the other configuration is proportional to the product $\boldsymbol{V}\boldsymbol{L}_k^{-1}\boldsymbol{V}^T$, where $\boldsymbol{L}_k^{-1}$ is the submatrix of order $K\times K$ taken in the upper left part of $\boldsymbol{L}^{-1}$, the inverse of $\boldsymbol{L}$. Using the elements of $\boldsymbol{L}^{-1}\boldsymbol{Y}$ it is possible to define the function:

$$f(x,y)=a_1+a_x+x_y+\sum_{i=1}^{K}W_iU(|Z_i-(x,y)|),$$

where $f(x_i,y_i)=v_i$ permits to interpolate the correspondence between both series of homologous points (Z_i and Z'_i). The product $\boldsymbol{V}\boldsymbol{L}_k^{-1}$ gives the coefficients for the non-affine part of the transformation (W_i) and the affine coefficients (a_1, a_x, x_y) are given by $\boldsymbol{V}\boldsymbol{L}_Q^{-1}$,

where $\boldsymbol{L}_Q^{-1}$ is the submatrix of order $K \times 3$ taken in the upper right part of $\boldsymbol{L}^{-1}$. The application of $\boldsymbol{L}_k^{-1}$ and $\boldsymbol{L}_Q^{-1}$ on the first row of V specifies the non-affine and affine coefficients, respectively, for the x-coordinates, and its application to the second row gives the corresponding coefficients for y-coordinates. The net bending energy is then calculated by adding the energies for bending both in x and y-axes.

The bending energy matrix is decomposed as $\boldsymbol{L}_k^{-1} = EAE^T$, where A is a diagonal matrix of order $K \times K$ with the associated eigenvalues and E is a matrix $K \times K$ which includes the eigenvectors (whose columns are the normalized vectors and its rows the selected landmarks). The eigenvectors -or principal components- of the matrix $\boldsymbol{L}_k^{-1}$ are named principal warps; this matrix has the three latter components with eigenvalues of zero, because they correspond to landmark displacements in affine transformations (translation, rotation and dilation), which require no energy.

The principal warps may be drawn in diagrams, one for each warp, which represent their effect on the configuration of original landmarks and are then interpretable as distinct patterns of landmark displacements in the plane that contains the figure (partial warps). The non-uniform transformation consists of the algebraic addition of partial warps, and joined with the affine component, they both represent the total warp. The bending energy value associated with each principal warp is inversely proportional to the magnitude of its eigenvalue, because the greater eigenvalues correspond to eigenvectors which describe characteristics of lower order in the change of form (i.e. non-affine displacements for distantly spaced landmarks).